Propagation of errors from shore baselines seaward

Petr Vaníček
Department of Geodesy and Geomatics Engineering
University of New Brunswick
Fredericton, N.B., Canada

Abstract

All maritime boundaries are defined by turning points and by straight lines or curves connecting these points. The points can be positioned only to a limited accuracy. That accuracy is normally shown by two-dimensional confidence limits, also known as error ellipses. These confidence limits can be thought of as portraying the areas of positional uncertainty. The main problem we investigate in this paper is: What is the uncertainty in the line (baseline) connecting two such uncertain positions? The corollary problem of probabilities associated with the uncertainties as well as the role of statistical dependence between baseline end-points are discussed. Then the impact of uncertainties in baselines on the maritime boundary is addressed. Some thought is given to the impact of boundary uncertainty on encroachment litigation.

Introduction

While positional uncertainties have always been considered in geodesy (in terms of covariance matrices and confidence regions), uncertainties in lines that connect two uncertain positions have received little attention. In this contribution, the latter problem is addressed with the goal of deriving a rigorous (as rigorous as statistics allows us to get) expression for the line uncertainty when the two end positions are burdened with random errors. The problem of systematic errors is considered beyond the scope of this presentation.

It is shown that the line uncertainty (confidence region) should be depicted by an 'uncertainty belt'. The shape of the uncertainty belt is dictated by the positional uncertainties of the end points and the cross-covariance between the two positions. All this is shown by means of elementary mathematics and statistics, which should be easy to follow.

Further, the probability (statistical confidence level) associated with uncertainty belts of different width is discussed. It is demonstrated that this probability is a function of the multiple of standard deviations used in the construction of the uncertainty belt and of how the covariance matrices of the end points have been estimated.

Once the boundary uncertainty is known, it makes an eminent sense to ask about its impact on encroachment issues. It is shown that the encroachment can be viewed as strictly probabilistic problem.

Positional uncertainty

No position on the surface of the earth can be determined with an absolute accuracy and every (point) position contains errors. These errors belong to two broad families: systematic and random. Systematic errors are those that can be evaluated through analysing all the circumstances. For a discussion of systematic errors in positions and their effect on maritime boundary uncertainties the reader is referred to [Vaníček, 1998]. Here we shall concentrate on the random errors. Random errors are unpredictable; they can be described only statistically by

means of standard deviations (σ_x , σ_y) of coordinates x, y, and by the covariance σ_{xy} between them [Mikhail, 1976], for a specific probability level “p”.

The usual way of describing the random error in a position (x,y) is by the covariance matrix **C**,
assembled as

$$\mathbf{C} = \begin{bmatrix} \sigma_x^2 & \sigma_{xy} \\ \sigma_{xy} & \sigma_y^2 \end{bmatrix} . \qquad (1)$$

This matrix is a standard by-product of geodetic position estimation (computation) and should be routinely available for all desired positions. A covariance matrix (1) can be interpreted geometrically as describing a one-sigma error ellipse, known in statistics as the one-sigma confidence region [Mikhail, 1976] – see Fig.1.

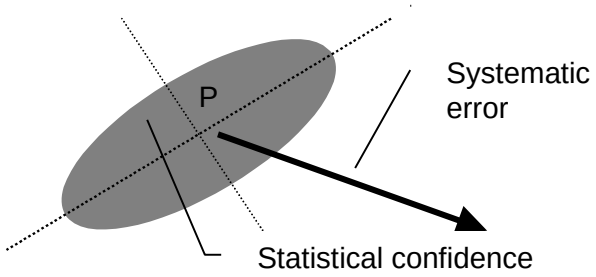

Figure 1- Position uncertainty

We shall be using, for the moment, the map coordinates (two-dimensional Cartesian coordinates x and y) to derive the uncertainties in the baselines. We shall show later how the results are applied to geodesics on the reference ellipsoid.

Uncertainty belt of a straight baseline

The question now arises: What will the uncertainty belt of a straight baseline that connects two points burdened with random errors look like? The situation is shown on Fig. 2. What we have to

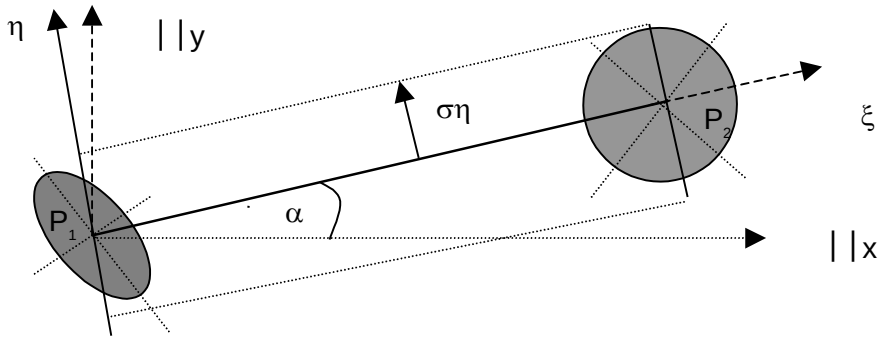

Figure 2 – Uncertainty belt of a straight baseline

investigate is the shape of the uncertainty (error) belt.

In the local coordinate system ξ,η at point P_1, the equation of the straight baseline is

$$\eta(\xi) = 0 . \tag{2}$$

The shape of the uncertainty belt can be described by the standard deviation of the coordinate η as a function of ξ, i.e., by $\sigma_\eta(\xi)$, which, in turn, will be a function of positional uncertainties in points P_1 and P_2, and their cross-covariances. Thus, to derive the expression for $\sigma_\eta(\xi)$, we have to have not only the covariance matrices $\mathbf{C}_1$ and $\mathbf{C}_2$ of points P_1 and P_2, but also their cross-covariance matrix $\mathbf{C}_{1,2}$ assembled as:

$$\mathbf{C}_{1,}{}^2 = \begin{bmatrix} \sigma_{x1,x2} & \sigma_{x1,y2} \\ \sigma_{y1,x2} & \sigma_{y1,y2} \end{bmatrix} . \tag{3}$$

The three matrices we need make up the (four by four) complete covariance matrix of the pair of points P_1 and P_2

$$\mathbf{C^*} = \begin{bmatrix} \mathbf{C}_1 & \mathbf{C}_{1,2} \\ \mathbf{C}_{2,1} & \mathbf{C}_2 \end{bmatrix} . \tag{4}$$

Such complete covariance matrix (of the vector $[x_1, y_1, x_2, y_2]^T$) is obtained as a by-product of the simultaneous estimation (computation) of the two positions and is, once more, routinely available for selected pairs of points. What we have to do now is to derive the expression for $\sigma_\eta(\xi)$ as a function of $\mathbf{C}^*$.

Let us begin by writing the equation for the baseline (eqn. (2)) in the x,y coordinate system. We get

$$y = a + b\,x = y_1 + \tan\alpha\ (x - x_1) , \tag{5}$$

where

$$a = y_1 - b\,x_1 , \quad b = \tan\alpha = (y_2 - y_1)/(x_2 - x_1) . \tag{6}$$

Next, we differentiate eqn. (5) to linearize the relation between x and y on the one hand and the four 'variables' $\mathbf{x} = [x_1, y_1, x_2, y_2]^T$, the errors in which we know (in terms of the covariance matrix $\mathbf{C}^*$):

$$dy = (\partial a/\partial \mathbf{x} + \partial b/\partial \mathbf{x}\, x)\, d\mathbf{x}\ , \tag{7}$$

where $\partial a/\partial \mathbf{x}$ and $\partial b/\partial \mathbf{x}$ are Jacobi's matrices composed of partial derivatives of scalars a and b with respect to the vector **x,** and d**x** is the differential vector

$$d\mathbf{x} = [dx_1, dy_1, dx_2, dy_2]^T\ . \tag{8}$$

The Jacobi matrices can now be evaluated. We get

$$\partial b/\partial \mathbf{x} = \mathbf{B} = \partial/\partial \mathbf{x}\left[(y_2 - y_1)/(x_2 - x_1)\right]\ , \tag{9}$$

$$\begin{aligned} \partial a/\partial \mathbf{x} = \mathbf{A} &= \partial\, y_1/\partial \mathbf{x} - b\, \partial\, x_1/\partial \mathbf{x} - \partial b/\partial \mathbf{x}\, x_1 \\ &= \partial\, y_1/\partial \mathbf{x} - b\, \partial\, x_1/\partial \mathbf{x} - \mathbf{B}\, x_1 \end{aligned} \tag{10}$$

and further

$$\mathbf{B} = [\tan\alpha, -1, \tan\alpha, -1]/(x_2 - x_1) = [\mathbf{D}\,|\,-\mathbf{D}]\ /(x_2 - x_1)\ , \tag{11}$$

$$\begin{aligned} \mathbf{A} &= [0,1,0,0] - b\,[1,0,0,0) - \mathbf{B}\, x_1 = [-b,1,0,0] - \mathbf{B}\, x_1 \\ &= [-\tan\alpha, 1,0,0] - \mathbf{B}\, x_1 = [-\mathbf{D}\,|\,\mathbf{0}] - [\mathbf{D}\,|\,-\mathbf{D}]\, x_1/(x_2 - x_1), \end{aligned} \tag{12}$$

where the symbol **D** stands for $[\tan\alpha, -1]$ and $|$ denotes matrix partitioning [Thompson, 1969]. Back substitution into eqn.(7) then yields

$$dy = \left\{[-\mathbf{D}\,|\,\mathbf{0}] + [\mathbf{D}\,|\,-\mathbf{D}]\ (x - x_1)/(x_2 - x_1)\right\} d\mathbf{x} \tag{13}$$

or, more simply,

$$dy = \left\{\mathbf{A}^* + \mathbf{B}^*\ (x - x_1)/(x_2 - x_1)\right\} d\mathbf{x}\ . \tag{14}$$

We may now realize that the argument $(x - x_1)/(x_2 - x_1) \in \langle 0,1\rangle$ can be also interpreted as running along the ξ-axis and we may thus replace it by

$$\xi^* = \xi / S_{1,2}\ , \tag{15}$$

where $S_{1,2}$ is the length of the baseline. Equation (14) then becomes

$$dy = (\mathbf{A}^* + \mathbf{B}^*\, \xi^*)\, d\mathbf{x}\ , \tag{16}$$

which is the equation that can be used for evaluating the systematic error in y from known systematic errors in **x**.

As we are here interested in random errors, we have to use the law of variance propagation [Vaníček and Krakiwsky, 1986] to see how the variances (squares of standard deviations) and covariances in the two end positions affect the variance of y. We get

$$\sigma_y^2(\xi^*) = (\mathbf{A}^* + \mathbf{B}^*\, \xi^*)\, \mathbf{C}^*\, (\mathbf{A}^* + \mathbf{B}^*\, \xi^*)^T \tag{17}$$

and, after the algebraic operations,

$$\sigma_y^2(\xi^*) = \mathbf{A}^*\mathbf{C}^*\mathbf{A}^{*T} + 2\, \mathbf{A}^*\mathbf{C}^*\mathbf{B}^{*T}\, \xi^* + \mathbf{B}^*\mathbf{C}^*\mathbf{B}^{*T}\, \xi^{*2}\ . \tag{18}$$

We now substitute for **A*, B*** and **C*** to get

$$\sigma_y^2(\xi^*) = \mathbf{D}\,\mathbf{C}_1\,\mathbf{D}^T - 2(\mathbf{D}\,\mathbf{C}_1\,\mathbf{D}^T - \mathbf{D}\,\mathbf{C}_{1,2}\,\mathbf{D}^T)\,\xi^* + (\mathbf{D}\,\mathbf{C}_1\,\mathbf{D}^T - 2\,\mathbf{D}\,\mathbf{C}_{1,2}\,\mathbf{D}^T + \mathbf{D}\,\mathbf{C}_2\,\mathbf{D}^T)\,\xi^{*2}$$
$$= \mathbf{D}\,[\mathbf{C}_1 - 2(\mathbf{C}_1 - \mathbf{C}_{1,2})\,\xi^* + (\mathbf{C}_1 - 2\,\mathbf{C}_{1,2} + \mathbf{C}_2)\,\xi^{*2}]\,\mathbf{D}^T \quad . \tag{19}$$

Let us write the **D** matrix in a slightly different form:

$$\mathbf{D} = [\tan\alpha, -1] = [\sin\alpha, -\cos\alpha] / \cos\alpha = \mathbf{S} / \cos\alpha \quad . \tag{20}$$

Substitution into eqn.(19) then yields

$$\sigma_y^2(\xi^*) = \mathbf{S}\,[\mathbf{C}_1 - 2(\mathbf{C}_1 - \mathbf{C}_{1,2})\,\xi^* + (\mathbf{C}_1 - 2\,\mathbf{C}_{1,2} + \mathbf{C}^2)\,\xi^{*2}]\,\mathbf{S}^T / \cos\alpha \; . \tag{21}$$

We have derived the equation for $\sigma_y^2(\xi^*)$; what remains to be done is to transform it into $\sigma_\eta^2(\xi^*)$ and we are done. As the angle between the (x,y) and the (ξ,η) coordinate system is α, the transformation between differential vectors $d\mathbf{r}_x$ and $d\mathbf{r}_\xi$ is given by

$$d\mathbf{r}_\xi = \mathbf{R}(\alpha)\,d\mathbf{r}_x \; , \tag{22}$$

where $\mathbf{R}(\alpha)$ is the rotation matrix [Vaníček and Krakiwsky, 1986] which rotates one coordinate system into the other. An application of the variance propagation law then gives

$$\mathbf{C}_\xi = \mathbf{R}(\alpha)\,\mathbf{C}_x\,\mathbf{R}^T(\alpha) = \mathbf{R}(\alpha)\,\mathbf{C}\,\mathbf{R}^T(\alpha) \quad , \tag{23}$$

and we get for the variance in the η-direction

$$\sigma_\eta^2 = \sigma_x^2 \sin^2\alpha - 2\,\sigma_{x,y} \sin\alpha \cos\alpha + \sigma_y^2 \cos^2\alpha \quad . \tag{24}$$

We note that the locus of distances σ_η (or equivalently, the locus of σ_ξ) around a point is known in geodesy as the pedal curve [Vaníček and Krakiwsky, 1986]. In our application $\sigma_x^2 = \sigma_{x,y} = 0$, as x is the independent variable, and we get

$$\sigma_\eta^2 = \sigma_y^2 \cos^2\alpha \quad . \tag{25}$$

Substitution back in eqn.(21) yields the final expression we have been seeking

$$\sigma_\eta^2(\xi^*) = \mathbf{S}\,[\mathbf{C}_1 - 2(\mathbf{C}_1 - \mathbf{C}_{1,2})\,\xi^* + (\mathbf{C}_1 - 2\,\mathbf{C}_{1,2} + \mathbf{C}^2)\,\xi^{*2}]\,\mathbf{S}^T \quad . \tag{26}$$

Note that the variance σ_η^2, i.e., the square of the uncertainty belt width, is a quadratic function of ξ. It is easy to see that for $\xi^* = 0$ (point P_1) and $\xi^* = 1$ (point P_2), we obtain the correct values of σ_η^2 that we would get directly from $\mathbf{C}_1$ and $\mathbf{C}_2$.

To close this section, let us have another look at eqn.(16). It can be easily transformed into the following form

$$d\eta = \mathbf{S}[(1 - \xi^*)\,d\mathbf{x_1} + \xi^*\,d\mathbf{x_2}] \; , \tag{27}$$

and, replacing the differentials with systematic errors denoted by ε, we get

$$\varepsilon_\eta = \mathbf{S}[(1 - \xi^*)\,\boldsymbol{\varepsilon_1} + \xi^*\,\boldsymbol{\varepsilon_2}] \; , \tag{28}$$

the equation that describes the effect of systematic errors $\boldsymbol{\varepsilon_1}$, $\boldsymbol{\varepsilon_2}$ in the end-point positions on the width of the uncertainty belt. We note that the effect is a linear function of ξ.

A closer look at the uncertainty belt

Let us now have a closer look at eqn.(26). Not surprisingly, we discover that the shape of the uncertainty belt is controlled by the cross-covariance matrix $\mathbf{C}_{1,2}$ for the two end points. We have the following three extreme cases:

1. For the <u>total statistical independence</u> of the two positions (this situation occurs when the two end points had been positioned completely independently), which is characterised by $\mathbf{C}_{1,2} = \mathbf{0}$, eqn.(26) reduces to

$$\sigma_\eta^2(\xi^*) = \mathbf{S}\,[\mathbf{C}_1 - 2\mathbf{C}_1\,\xi^* + (\mathbf{C}_1 + \mathbf{C}_2)\,\xi^{*2}]\,\mathbf{S}^T \quad , \tag{29}$$

which can be further simplified to

$$\sigma_\eta^2(\xi^*) = \sigma_{\eta 1}^2 - 2\,\sigma_{\eta 1}^2\,\xi^* + (\sigma_{\eta 1}^2 + \sigma_{\eta 2}^2)\,\xi^{*2} \quad . \tag{30}$$

Take, for simplicity, the same variance $\sigma_{\eta 1}^2$ at both ends of the baseline. We get

$$\sigma_\eta(\xi^*) = \sigma_{\eta 1}\,\sqrt{(1 - 2\,\xi^* + 2\,\xi^{*2})} = \sigma_{\eta 1}\,Q(\xi^*) \tag{31}$$

and the shape $Q(\xi^*)$ is a square root of a quadratic function of ξ^*. The ordinate at the mid point is equal to 0.707.

2. For two <u>totally positively statistically dependent</u> positions (this situation occurs, for example, when one position is determined relative to the other position with very high relative accuracy) typified by $\mathbf{C}_{1,2} = \mathbf{C}_1^{1/2}\mathbf{C}_2^{1/2}$, considering again the same accuracy at both ends ($\mathbf{C}_{1,2} = \mathbf{C}_1 = \mathbf{C}_2$), eqn.(26) reduces to

$$\sigma_\eta(\xi^*) = \sigma_{\eta 1} \, . \tag{32}$$

The standard deviation in η is then a constant function of ξ. Generally, for two totally positively statistically dependent positions, the uncertainty belt is delimited by straight lines.

3. For two <u>totally negatively statistically dependent</u> positions (this situation is only of an academic interest as it cannot occur in practice) and considering again the same accuracy at both ends, eqn.(26) becomes

$$\sigma_\eta(\xi^*) = \sigma_{\eta 1}\,\sqrt{(1 - 4\,\xi^* + 4\,\xi^{*2})} = \sigma_{\eta 1}\,Q'(\xi^*) \, . \tag{33}$$

The shape of the belt, $Q'(\xi^*)$, is again a square root of a quadratic function. This time, however, the ordinate at the mid point goes to 0.

The three extreme cases are shown in Fig.3. We note that any real case will fall probably

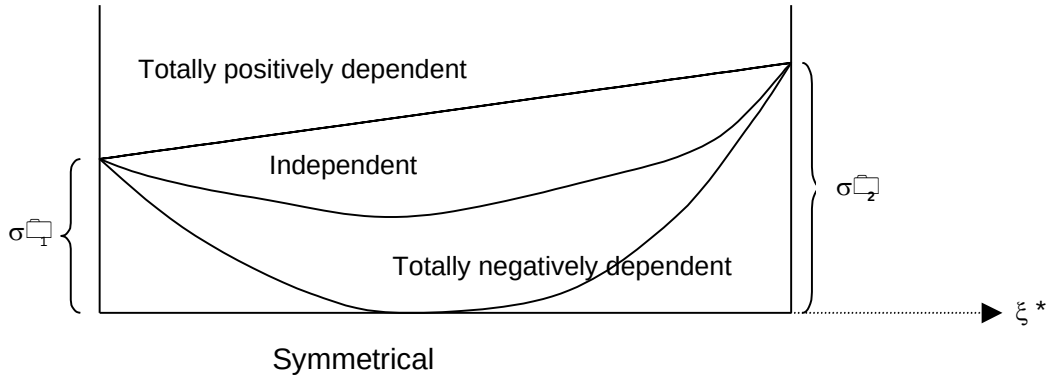

Figure 3 – The shape of uncertainty belt

somewhere between the total positive dependence and the total independence. An example of a real uncertainty belt for a straight baseline is shown in Fig. 4.

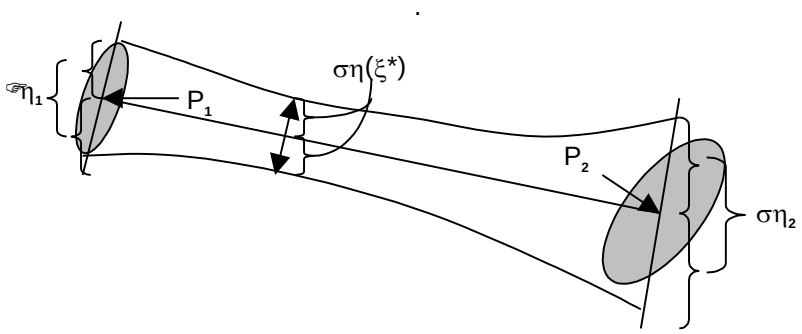

Figure 4 – Complete uncertainty belt

Probabilistic issues

What is the probability of the actual straight baseline being within the uncertainty belt computed according to eqn. (26)? The one-standard-deviation uncertainty belt we have constructed above is associated with the same probability p as the two standard deviations at the ends of the baseline imply. This probability, in turn, depends on how the scale σ_0 of the covariance matrix **C*** [Vaníček and Krakiwsky, 1986] had been determined. The way the scale, known as the variance factor, had been determined dictates the probability density function (PDF) which governs the whole probabilistic consideration.

We can be dealing with any one of the following three PDFs:

1. Normal PDF (n), which is applicable when the variance factor σ_0 was known independently;
2. Pope's τ PDF, applicable when σ_0 had been estimated during the computation of the end positions;
3. Student's t PDF, applicable when σ_0 had been estimated from a different experiment (from different measurements).

The three probabilities, associated with the three PDFs, obey the following inequalities:

$$p_n > p_t > p_\tau \ . \qquad (34)$$

If an uncertainty belt of a specified probability, also called confidence level in statistic, is desired then an appropriate multiple of $\sigma_\eta(\xi^*)$ is used. Fig. 5 shows how this idea works for the

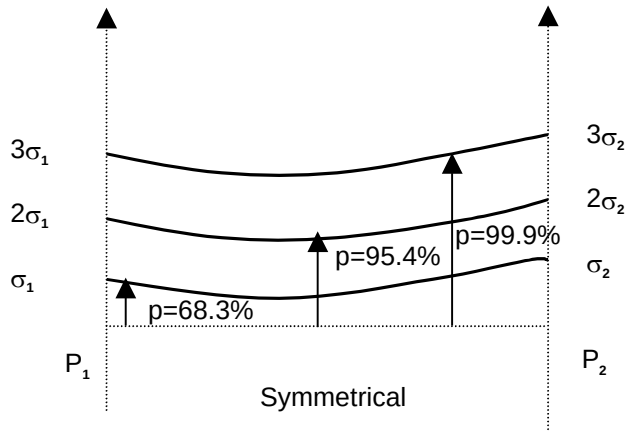

Figure 5 – Probabilities associated with multiples of standard deviations

known σ_0 , i.e., for the normal PDF (and for $\mathbf{C}_{1,2} = \mathbf{0}$). Naturally, different '$k\sigma_\eta$ - belts' will have different confidence levels for different PDFs.

Geodesic curve as a straight baseline

Generally, a geodesic curve on the reference ellipsoid appears on the map as a curve and not as a straight line. We speak of the projected geodesic. A typical situation is shown on Fig.6. Since most of the time, the 'straight baselines' are defined as geodesics on the reference

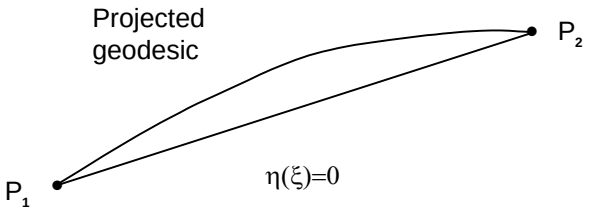

Figure 6 – Geodesic curve on the reference ellipsoid projected on the mapping plane

ellipsoid, this is the situation we will face. Let us just note that while the curved line is an image of the geodesic connecting points P_1 and P_2 on the reference ellipsoid, the straight line $\eta(\xi) = 0$ is the geodesic connecting points P_1 and P_2 on the mapping plane.

To get the uncertainty belt on the reference ellipsoid we simply calculate two curves on either side of the geodesic with + or - $k\sigma_\eta(\xi)$ offset. The result is illustrated in Fig. 7. We note,

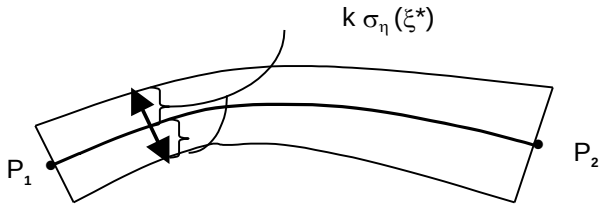

Figure 7 – Geodesic curve as a baseline

That the borders of the uncertainty belt on the ellipsoid are no longer geodesic curves.

Seaward extension

When straight baselines are extended seaward by a specific number (m) of nautical miles, the +/- $k\sigma_\eta(\xi)$-belts remain the same. For the circular portions of the sea boundary, the uncertainty belt must be calculated from the positional uncertainty (i.e., the covariance matrix **C)** of the point around which the circle is drawn. The expression for the uncertainty σ_ξ is computed again from eqn.(23). We obtain (cf. eqn.(24))

$$\sigma_\xi^2 = \sigma_x^2 \cos^2\alpha + 2\,\sigma_{x,y} \sin\alpha \cos\alpha + \sigma_y^2 \sin^2\alpha \ . \qquad (35)$$

The situation is shown on Fig.8.

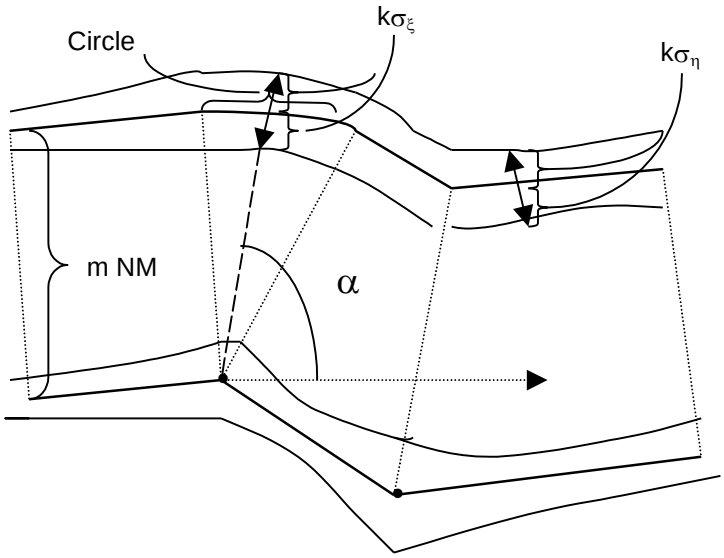

Figure 8 – Extension Seaward

Clearly, the uncertainty belt constructed around a boundary extended from land straight baselines is likely to be quite narrow. As the baselines are connecting land-based points, which are apt to have been determined to a fairly high accuracy, we may expect the width of the +/- $k\sigma_\eta(\xi)$-belt to be typically in metres, after an appropriate care has been taken to eliminate the existing systematic errors [Vaníček, 1998]. However, a similar +/- $k\sigma_\eta(\xi)$-belt should be constructed also around a boundary extended from base points located either on the 2,500-metre isobath, or at the foot of the continental slope. The positional accuracy of these submersed base points will be much worse, perhaps by up to three orders of magnitude, and, consequently, the width of the uncertainty belt may be up to several kilometres wide.

Encroachment issues

The most important consequence of the boundary uncertainty is in the realm of encroachment. How does the uncertainty impact the act of encroachment? Put quite simply, an encroachment becomes a probabilistic issue! It should be possible to attach a probability to a statement “Party A is encroaching on state’s X territory”. This concept is illustrated in Fig.9. The

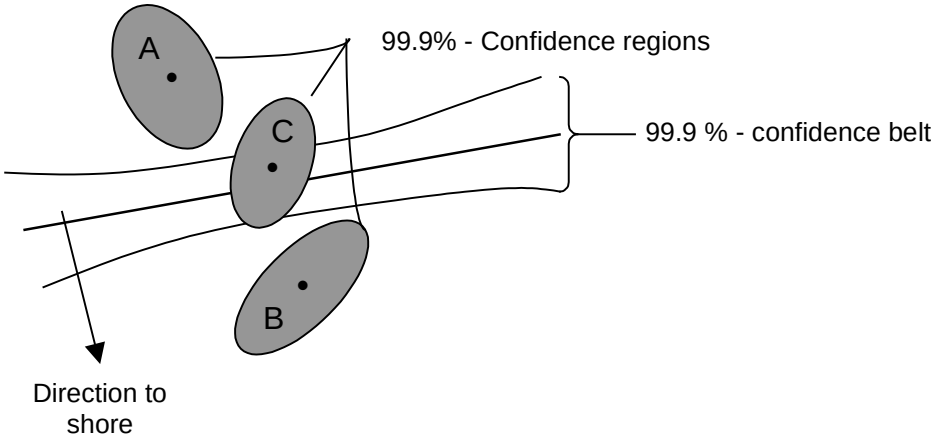

Figure 9 - Encroachment

figure shows a boundary with its uncertainty belt, the positions of the potential encroachers and the positional uncertainties of these positions. It is easy to see that in this illustration, the probability of party A encroaching on X's territory is practically nil. Conversely, the probability of B encroaching is practically equal to 1, i.e., party B is certainly encroaching. The answer is not clear cut in the case of party C.

In reality, the situation is even more complicated. In addition to the position determined by the potential encroacher there is the position (of the potential encroacher) as determined by the potentially injured country. In Fig.10, A is the position determined by encroacher and A' is the

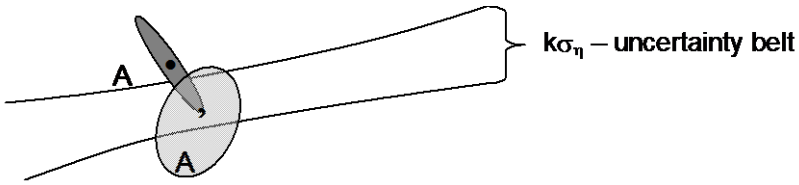

Figure 10 – Real situation

position determined by the injured country. The two positions as shown are statistically compatible on a probability level that can be evaluated from the overlap of the confidence regions. What is now the probability that party A is encroaching?

Conclusions

We have derived the rigorous expressions for the uncertainty in a maritime boundary caused by random errors in position determination and suggested how this uncertainty can be quantified, and shown on the reference ellipsoid or on a map, for a desired level of probability. We have also pointed out that, once the uncertainty is quantified, it is possible to determine the specific probability with which an encroachment occurs. Finally, we have pointed out that in practice the situation is more complicated by the fact that there would be two 'competing' position determinations, one by the potential encroacher and one by the potentially injured country. Working out the involved probabilistic estimates was, however, considered to be outside the scope of this contribution.

It is recommended that the probabilistic estimates be investigated in detail and the legal connotations be tested in court.

References

Mikhail, E.M., 1976. *Observations and Least Squares.* IEP-A dun-Donnelley Publisher.

Thompson, E.H., 1969. *An Introduction to the Algebra of Matrices with some Applications.* University of Toronto Press.

Vaníček, P., 1998. On the errors in the delimitation of maritime spaces. *International Hydrographic Review*, LXXV(1), March, pp.59-64.

Vaníček, P. and E.J. Krakiwsky, 1986. *Geodesy: the Concepts* – second edition, North Holland.